



HAL
open science

The Nature of Hypermassive Objects at the Center of M87 and the Milky Way

Hicham Zejli, Florent Margnat, Jean-Pierre Petit

► **To cite this version:**

Hicham Zejli, Florent Margnat, Jean-Pierre Petit. The Nature of Hypermassive Objects at the Center of M87 and the Milky Way. 2024. hal-04621388v3

HAL Id: hal-04621388

<https://hal.science/hal-04621388v3>

Preprint submitted on 11 Jul 2024

HAL is a multi-disciplinary open access archive for the deposit and dissemination of scientific research documents, whether they are published or not. The documents may come from teaching and research institutions in France or abroad, or from public or private research centers.

L'archive ouverte pluridisciplinaire **HAL**, est destinée au dépôt et à la diffusion de documents scientifiques de niveau recherche, publiés ou non, émanant des établissements d'enseignement et de recherche français ou étrangers, des laboratoires publics ou privés.

The Nature of Hypermassive Objects at the Center of M87 and the Milky Way.

H. Zejli¹, F.Margnat², J.P.Petit³

Keywords : giant black hole, hypermassive object, M87, Sgr A*, Geometric criticality, physical criticality, plugstar, internal metric, Flamm meridian surface, time factor, variable speed of light, Hoag galaxy, quasar.

Abstract : Focusing on the Sgr A* and M87 images of hypermassive objects at the center of M87, we note a divergence from an identification with images of giant black holes, as well as the identity, in both cases, of the value 3, representing the ratio of maximum to minimum temperature. It is suggested that these are subcritical objects, where the darkening of their central part derives from the fact that their radius is $(8/9)^{1/2}$ Rs. Under these conditions, a very strong pressure gradient can oppose the force of gravity. We suggest a scheme for the formation of your objects.

1 – Introduction

The kinematics of the objects orbiting the central part of the M87 and Milky Way galaxies are sufficiently well documented that the mass values responsible for such observations cannot be questioned. Nevertheless, when the first images appeared, in 2019[1] and 2022 [2], magazines headlined "Shadow of Giant Black Holes". The only reason given was that no other interpretation was possible. But the central parts of these objects are far from black.

¹ hicham.zejli@manaty.net

² florent.margnat@univ-poitiers.fr

³ jean-pierre.petit@manaty.fr

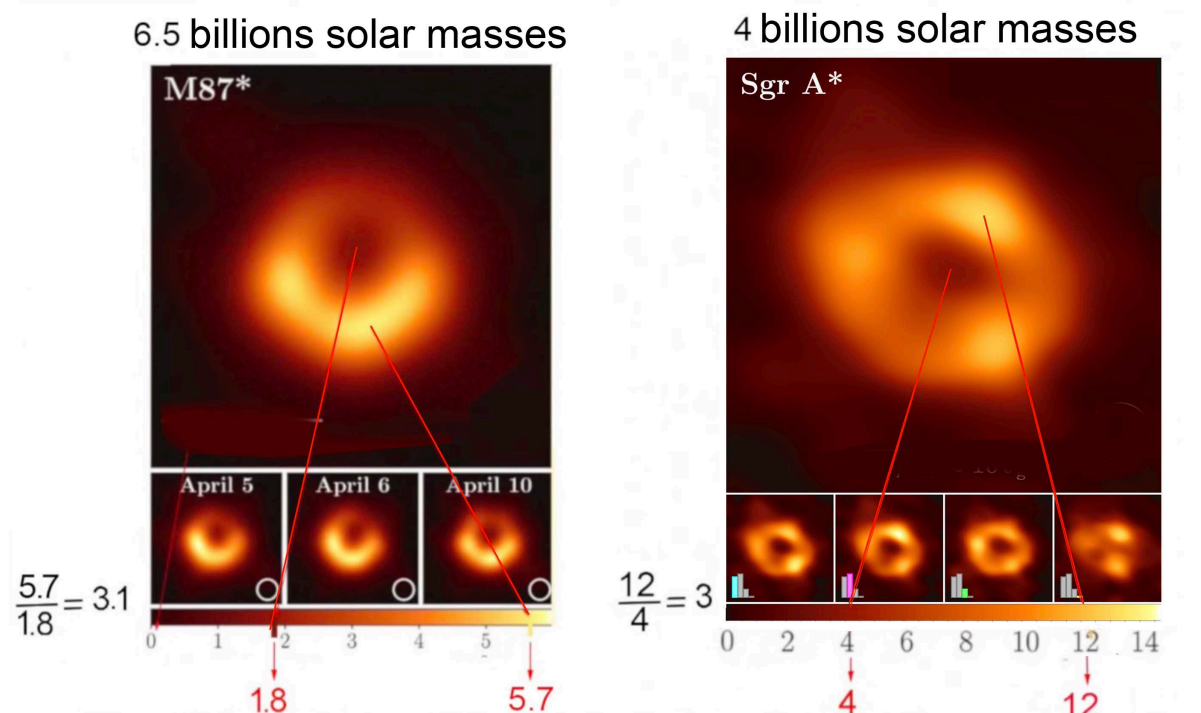


Fig.1 : Images of hypermassive objects at the center of M87 and the Milky Way.

If it's perhaps problematic to give credence to the temperature values displayed, we can evaluate the ratio of maximum and minimum temperatures in each image and find values very close to 3. Some have tried to justify this central temperature by the presence of the hot accretion disk in the foreground. But why doesn't it reveal its presence in the vicinity of the object? In [3], an attempt was made to reconstruct the characteristics of the “most likely black hole”, giving what we would expect to see if the presence of hot gas in the background did not interfere with the observation:

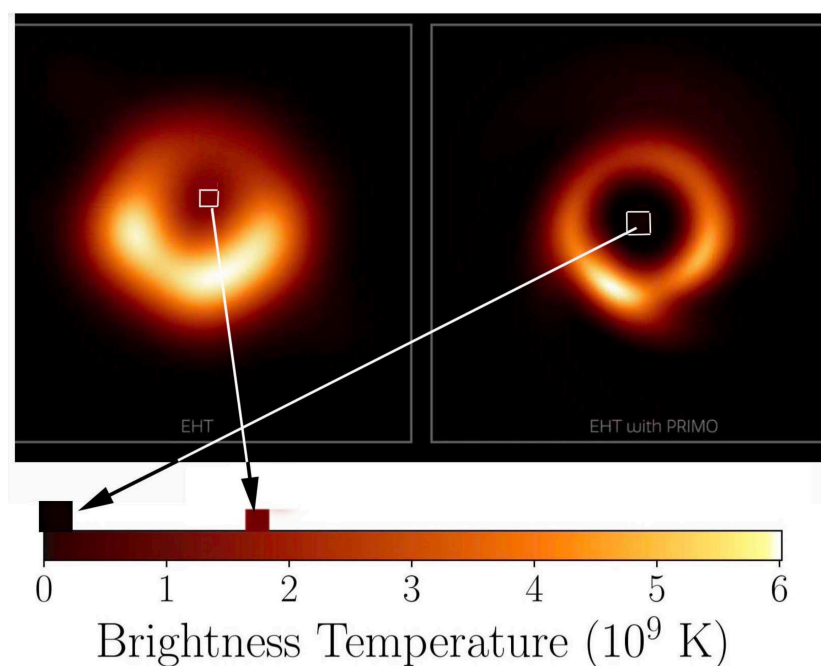


Fig.2 : Image reconstruction [3]

2 - Identification with subcritical objects.

That's one way of interpreting observations. Another is to stick strictly to the available data. We can then link the darkening of the central part to a gravitational redshift effect. Under these conditions, we can deduce the relationship between the object's radius and the corresponding value of the Schwarzschild radius related to its mass:

$$(1) \quad \frac{\lambda'}{\lambda} \approx 3 = \frac{1}{\sqrt{1 - \frac{8}{9}}} = \frac{1}{\sqrt{1 - \frac{2GM}{c^2 R_a}}}$$

The object could therefore be a subcritical object, as described by Karl Schwarzschild in his second paper [4], describing the geometry inside a sphere filled with an incompressible fluid of constant density. In [5], we find the shape of the pressure curve, which tends towards infinity at the center, when this critical situation is reached.

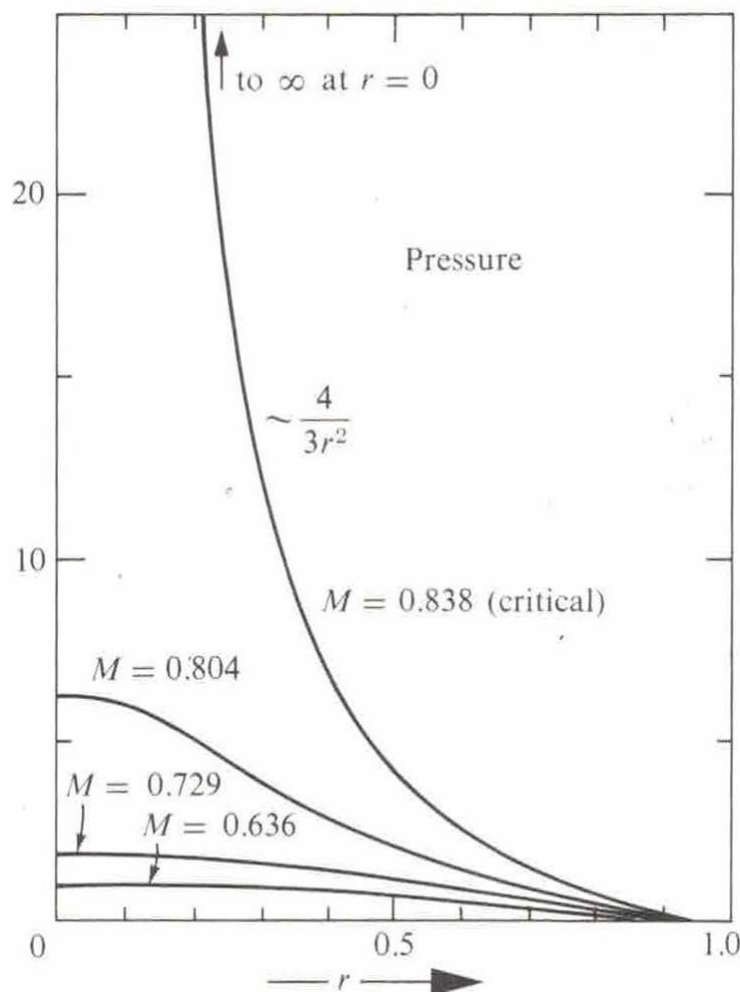


Fig.3 : Pressure trend [5].

If we assimilate these hypermassive objects to perfect gases, the pressure, assuming that the matter density ρ is constant, or varies little, represents a measure of the volumetric density of thermal agitation energy, with a velocity v :

$$(2) \quad p = \frac{\rho \langle v^2 \rangle}{3}$$

Going back in time, the Big Bang model shows a succession of increasingly dense and hot states. The dominant pressure soon becomes radiation pressure.:

$$(3) \quad p_r = \frac{\rho_r c^2}{3}$$

To take this further, it is necessary to consider that the speed of light can be considered as variable, under extreme conditions. In [5], we refuse to consider that this pressure surge has a physical character, arguing that the speed of sound in this medium would then exceed that of light, considered as an absolute constant. In his article of February 1916 [4], however, K. Schwarzschild considers this possibility. Within the mass, he uses an angular coordinate χ and a characteristic radius \hat{R} such that :

$$(4) \quad \hat{R} = \sqrt{\frac{3c_0^2}{8\pi G \rho}} \quad R = \hat{R} \sin \chi$$

The value c_0 then refers to the speed of light outside the object. The interior metric is then written :

Das Linienelement im Innern der Kugel nimmt, wenn man statt x_1, x_2, x_3 (ix) die Variablen χ, ϑ, ϕ benutzt, die einfache Gestalt an:

$$ds^2 = \left(\frac{3 \cos \chi_0 - \cos \chi}{2} \right)^2 dt^2 - \frac{3}{\alpha \rho_0} [d\chi^2 + \sin^2 \chi d\vartheta^2 + \sin^2 \chi \sin^2 \vartheta d\phi^2]. \quad (35)$$

Außerhalb der Kugel bleibt die Form des Linienelements dieselbe, wie beim Massenpunkt:

$$ds^2 = \left(1 - \frac{\alpha}{R} \right) dt^2 - \frac{dR^2}{1 - \alpha/R} - R^2 (d\vartheta^2 + \sin^2 \vartheta d\phi^2) \quad (36)$$

wobei:

$$R^3 = r^3 + \rho$$

ist. Nur wird ρ nach (33) bestimmt, während für den Massenpunkt $\rho = \alpha^3$ war.

Fig.4 : The Schwarzschild interior metric [4]

The continuity is ensured with the external metric, given below. The author, with $c_0 = 1$, gives the variation of the volumetric density of energy, of which pressure is a part, inside the object.

so verwandeln sich die Gleichungen (13), (26), (10), (24), (25) durch elementare Rechnung in die folgenden:

$$f_2 = \frac{3}{\kappa \rho_0} \sin^2 \chi, \quad f_4 = \left(\frac{3 \cos \chi_a - \cos \chi}{2} \right)^2, \quad f_1 f_2 f_4 = 1. \quad (29)$$

$$\rho_0 + p = \rho_0 \frac{2 \cos \chi_a}{3 \cos \chi_a - \cos \chi} \quad (30)$$

$$3x = r^3 = \left(\frac{\kappa \rho_0}{3} \right)^{-3/2} \left[\frac{9}{4} \cos \chi_a \left(\chi - \frac{1}{2} \sin 2\chi \right) - \frac{1}{2} \sin^3 \chi \right]. \quad (31)$$

Die Konstante χ_a bestimmt sich aus Dichte ρ_0 und Radius r_a der Kugel

Fig.5 : Evolution of total pressure inside the object [4]

As Schwarzschild noted over a century ago, this imposes the constraint $\cos \chi < 1/3$. L.Flamm gave [6] a description of the geometry of the set by producing the meridian curve corresponding to the section of the 4D object, first by planes $t = cst$ then by planes $\theta = cst$. He then obtained the following:

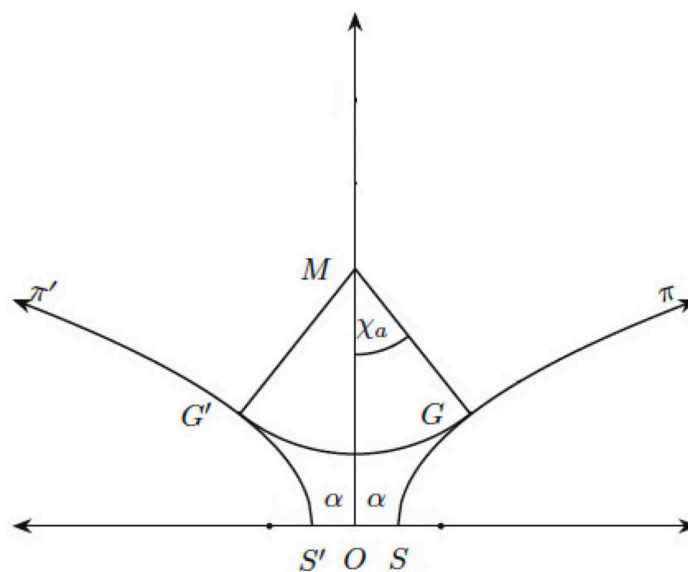


Fig.6 : Meridian by L.Flamm [6]

The $SO(3)$ -invariant solution to Einstein's equation corresponds to a 3D object translating along the time coordinate. This object is made up of two connected sets. The first is a portion of the hypersphere S^3 , with radius of curvature \hat{R} . The second is a portion of a Flamm hypersurface whose meridian is a lying parabola. Two criticalities thus emerge. The first is that envisaged by proponents of black hole theory. The conditions then become such that $R_a = \hat{R}$ ($\chi = \pi/2$). We'll call this "geometric criticality". The meridian then becomes :

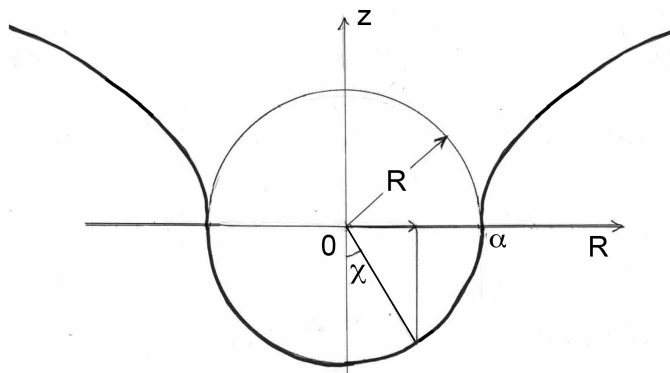


Fig.7 : Geometric criticality.

But even before this "geometrical criticality" occurs, the "physical criticality" mentioned by Schwarzschild [4] comes into play, corresponding to an χ angle value close to $\pi/3$. We reproduce below the portion of the meridian curve given in [5].

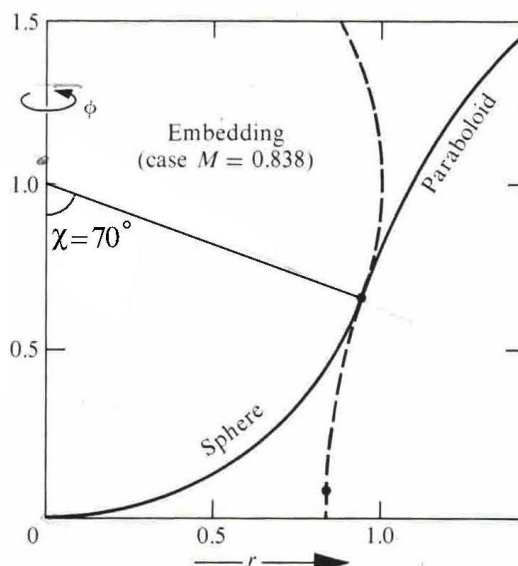


Fig.8 : Physical criticality. Meridian [5]

If we retain this idea of a steep rise in the value of the speed of light inside the object, the corresponding pressure gradient is therefore able to oppose the force of gravity. In his article, Schwarzschild denotes the time coordinate by x_4 and the corresponding coefficient of his metric by f_4 :

einzuführen. Das Linienelement muß dann, wie dort, die Form haben :

$$ds^2 = f_4 dx_4^2 - f_1 dx_1^2 - f_2 \frac{dx_2^2}{1-x_2^2} - f_2 dx_3^2 (1-x_2^2), \quad (8)$$

so daß man hat :

Fig.9 : Schwarzschild line element [4].

This coefficient is referred to in the literature [5] as the square of a so-called time factor. Schwarzschild gives its evolution according to:

SCHWARZSCHILD: Über das Gravitationsfeld einer Kugel

427

Das läßt sich sofort integrieren und gibt:

$$(\rho_0 + p) \sqrt{f_4} = \text{konst.} = \gamma. \quad (10)$$

Die Feldgleichungen (a) (b) (c) lassen sich durch Multiplikation mit

Fig.10 : Time factor evolution after Schwarzschild [4].

It can be seen that this time factor tends towards zero when physical criticality conditions are reached. In the figure below, we show the evolution of this time factor, for different mass values:

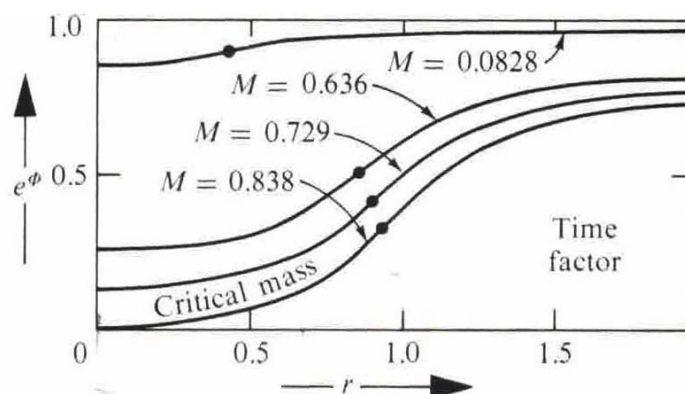


Fig.11 : Evolution of the time factor for different mass values [5]

The authors [5] limited themselves to the value of critical mass. But let's see what happens when we push beyond it, what would happen if such an object suddenly benefited from a slight increase in mass:

time factor

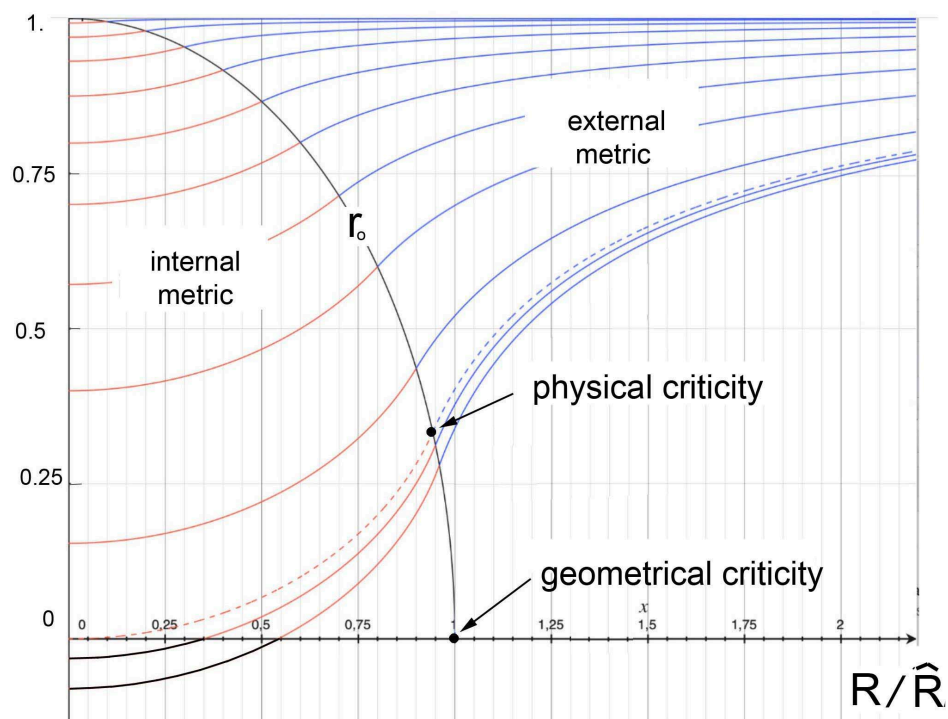


Fig.12 : Beyond physical criticality.

The time factor then becomes negative inside a small sphere centered on the origin, whose radius is growing extremely fast:

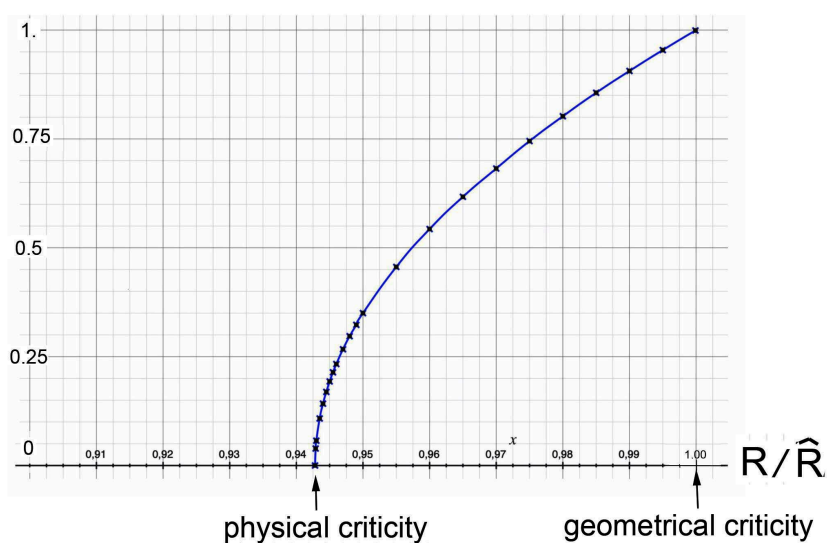


Fig.13 : Rapid expansion of the radius of the negative time factor region.

3 – A self-stability mechanism.

What is the significance of this negative time factor? The first to consider this possibility was H. Weyl, in 1917 [7]. He too presented the equation for the meridian of the hypersurface:

... im folgenden Rotationsparaboloid im Euklidischen Raum
 mit den rechtwinkligen Koordinaten x_1, x_2, z gilt:

$$z = \sqrt{8a(r-2a)},$$

 ... dasselbe durch orthogonale Projektion auf die Ebene
 $z=0$ mit den Polarkoordinaten r, ϑ bezogen wird. Die Pro...

Fig.14 : Weyl, meridian equation [7]

He was also the first to give an expression for the exterior metric using isotropic coordinates, and it was in this form that he envisaged the negative passage of the time-factor, for him on the Schwarzschild sphere ($r = a/2$).

dem Innern des Massenpunktes entsprechen. Bei analytischer
 Fortsetzung wird

$$\sqrt{f} = \frac{r - a/2}{r + a/2}$$

 im Innern negativ, so daß also dort für einen ruhenden Punkt

Fig.15 : Weyl time-factor, in isotropic coordinates [7].

For our purposes, this inversion of the time factor concerns the interior metric. Let's consider a stationary observer in this central region. The evolution of proper time corresponds to:

$$(5) \quad ds = (\text{time factor}) dt$$

The time factor, identified with the length s , cannot be reversed (you can't turn back along a geodesic). If geodesics are to be extended into the region where the time factor reverses, this can only be done by inverting the time coordinate t . Its inversion is now widely considered, as is the existence of a second T-symmetric universe ([8] to [13]). Theoretical physicists are now considering a possible interaction between these two folds by "entanglement", which would then justify the acceleration of the universe's expansion. In [14], [15], this interaction is based on a two-folds configuration of the universe, the benefit

of which is also the acceleration of expansion [16]. This bimetric model is based on a system of two coupled field equations [17]:

$$(6) \quad R_{\mu}^{\nu} - \frac{1}{2}R g_{\mu}^{\nu} = \chi \left[T_{\mu}^{\nu} + \sqrt{\frac{g}{g}} \hat{T}_{\mu}^{\nu} \right]$$

$$(7) \quad \bar{R}_{\mu}^{\nu} - \frac{1}{2}\bar{R} \bar{g}_{\mu}^{\nu} = -\chi \left[\bar{T}_{\mu}^{\nu} + \sqrt{\frac{g}{\bar{g}}} \hat{\bar{T}}_{\mu}^{\nu} \right]$$

In the situation considered, considering for simplicity a situation where the determinants of the two metrics $g_{\mu\nu}$ and $\bar{g}_{\mu\nu}$ are equal, then $g_{\mu\nu}$ and $\bar{g}_{\mu\nu}$ metric solutions of the system :

$$(8) \quad R_{\mu}^{\nu} - \frac{1}{2}R g_{\mu}^{\nu} = \chi T_{\mu}^{\nu}$$

$$(9) \quad \bar{R}_{\mu}^{\nu} - \frac{1}{2}\bar{R} \bar{g}_{\mu}^{\nu} = -\chi \hat{\bar{T}}_{\mu}^{\nu}$$

The solution to equation (8) is represented by the pair of two metrics, inner and outer Schwarzschild, with coordinate:

$$(10) \quad ds^2 = \left[\frac{3}{2} \sqrt{1 - \frac{R_a^2}{\hat{R}^2}} - \frac{1}{2} \sqrt{1 - \frac{R^2}{\hat{R}^2}} \right]^2 dt^2 - \frac{dR^2}{1 - \frac{R^2}{\hat{R}^2}} - R^2 d\theta^2 - R^2 \sin^2 \theta d\phi^2$$

$$(11) \quad ds^2 = \left(1 - \frac{R^2}{\hat{R}^2} \right) dt^2 - \frac{dR^2}{1 - \frac{R^2}{\hat{R}^2}} - R^2 d\theta^2 - R^2 \sin^2 \theta d\phi^2$$

In the second sheet, under the conditions of the Newtonian approximation [17], we obtain with:

$$(12) \quad \hat{\bar{T}}_{\mu}^{\nu} = \begin{pmatrix} \rho & 0 & 0 & 0 \\ 0 & p & 0 & 0 \\ 0 & 0 & p & 0 \\ 0 & 0 & 0 & p \end{pmatrix}$$

the following line elements :

$$(13) \quad d\bar{s}^2 = \left[\frac{3}{2} \sqrt{1 + \frac{R_a^2}{\hat{R}^2}} - \frac{1}{2} \sqrt{1 + \frac{R^2}{\hat{R}^2}} \right]^2 dt^2 - \frac{dR^2}{1 + \frac{R^2}{\hat{R}^2}} - R^2 d\theta^2 - R^2 \sin^2 \theta d\phi^2$$

$$(14) \quad ds^2 = \left(1 + \frac{R^2}{\hat{R}^2} \right) dt^2 - \frac{dR^2}{1 + \frac{R^2}{\hat{R}^2}} - R^2 d\theta^2 - R^2 \sin^2 \theta d\varphi^2$$

Leading to geodesics that evoke repulsion. The situation becomes clearer. When matter is added, a passageway is created in the central part of the object. The masses found there move into the second sheet of the universe, with an inversion of the time coordinate, and therefore of the mass [18]. Following the geodesics of this second fold, this excess mass is then expelled from the object, in a mechanism that prevents a toilet from overflowing. We propose to call such subcritical objects plugstars:

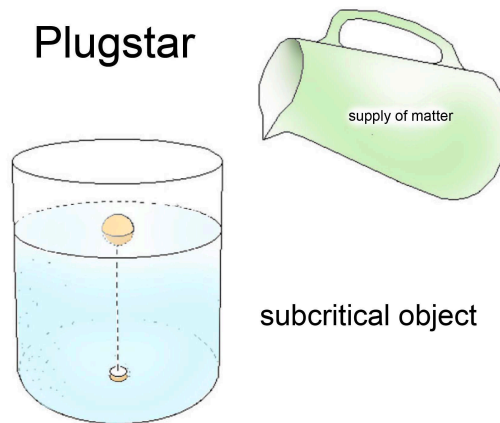


Fig.16 : Plugstar.

This model is opposed to the interpretation of images of hypermassive objects as giant black holes, but has the advantage of being consistent with observational data. It's quite remarkable that, while the masses and temperatures of these two objects differ significantly, their maximum/minimum temperature ratios are so close.

If the proposed model is correct, we conjecture that the same will be true for all future images of hypermassive objects.

4 – On the formation of hypermassive objects and quasars.

Until now, the idea was that these objects, considered to be giant black holes, must have formed by the merger of so-called stellar black holes. But the discovery of such hypermassive objects at an age of the universe of only a few hundred million years made this scenario difficult to envisage. The term primordial black holes was then suggested [19]. But the term "primordial" gives little information about how these objects would have formed. In the context of this bimetric model [17], we are currently studying a scenario in which joint fluctuations in metrics are involved. In this model, galaxy confinement is ensured not by positive-mass dark matter halos, but by the fact that these

galaxies are lodged in gaps forming in the negative-mass distribution. Joint fluctuations in metrics affect the "apparent mass factor" $\sqrt{\frac{|G|}{G}}$.

When it is weakened, the confinement loosens and the galaxy breaks up. This leads to the formation of irregular galaxies. When, on the other hand, the confinement factor is strengthened, a centripetal density wave is formed, of which the Hoag galaxy could be an example.

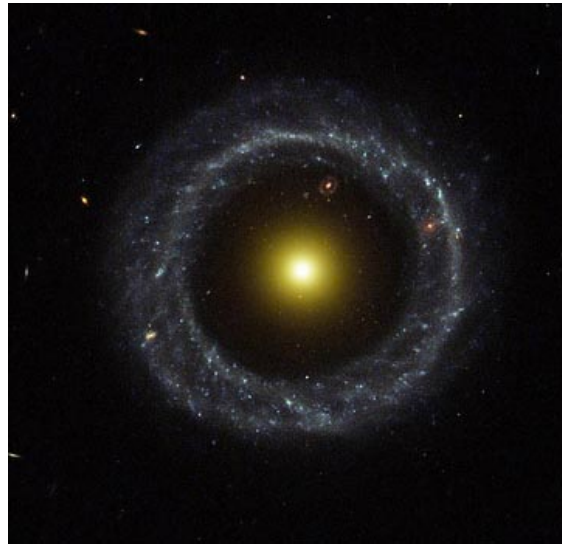


Fig.17 : Hoag galaxy

This density wave becomes stronger as it approaches the galactic center. As it passes, it gives rise to new stars, and it is the UV radiation it emits which, by exciting the gas, reveals its presence, as in the case of spiral waves. If the magnetic Reynolds number is locally high, the wave will pick up all the lines of force corresponding to the weak magnetic field pre-existing in the galaxy.

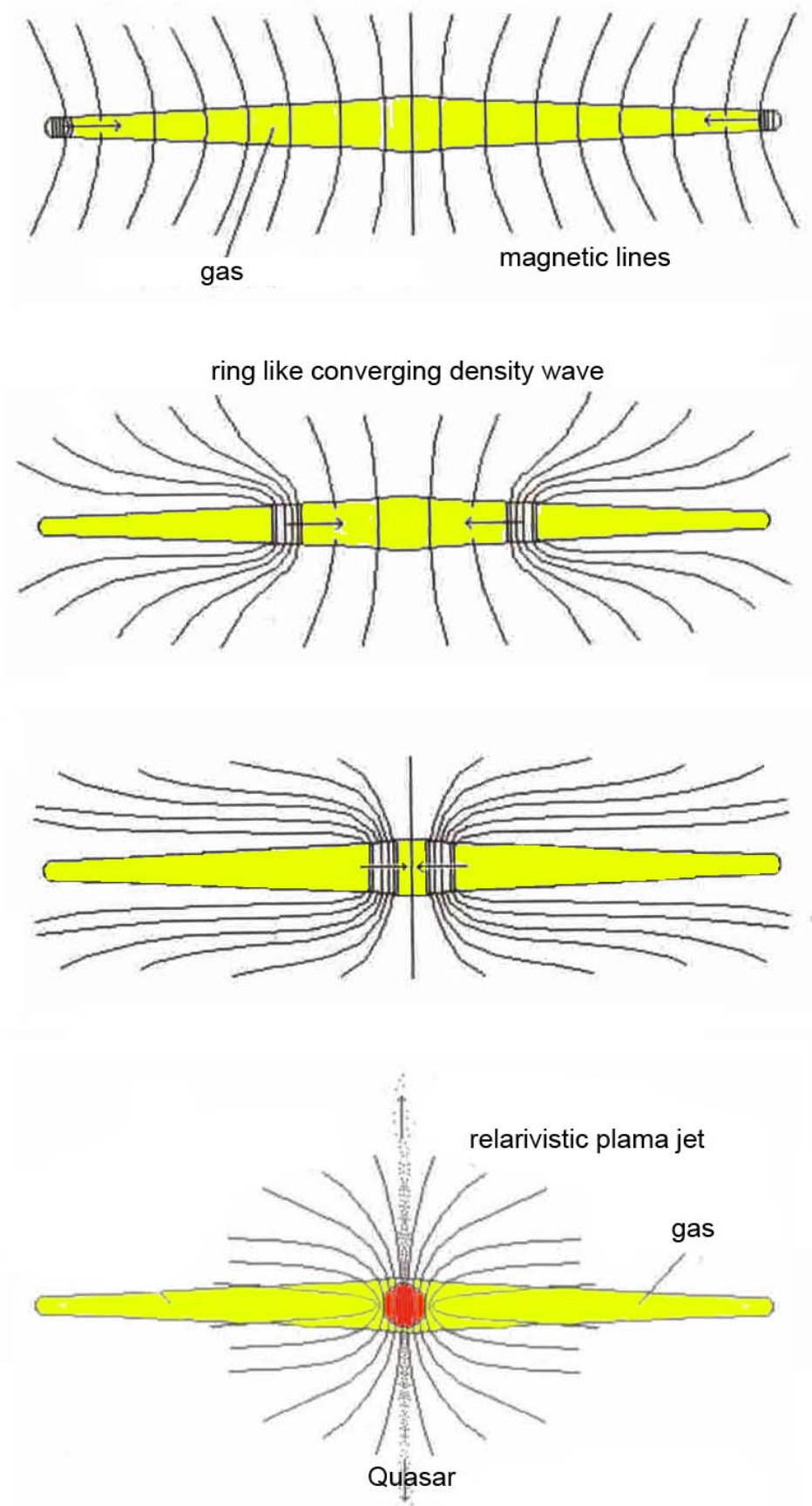


Fig. 17 : Quasar formation.

When convergence is complete, a hot, dense object is created at the center of the galaxy, where fusion reactions result in plasma emission, focused along the two lobes by the very powerful magnetic field. So that we get a quasar. The magnetic field gradient transforms these plasma jets into natural particle gas accelerators, birthplaces of cosmic rays. Excess mass is eliminated by the plugstar phenomenon, generating a powerful gravitational wave. This would correspond to the object at the center of galaxy M87. After a while, the plasma emission ceases. If fluctuations occur again, the mechanism resumes and plasma emission from the quasar is sporadic, as appears to be the case for 87. In a future article, we'll present the theory of joint metric fluctuations. What emerges is that the phenomenon is all the more important in that in the most primitive state of the universe, this last would be extremely agitated and turbulent. On the scale of a galaxy, density waves generate new stars. But on a much larger scale, galaxy rings are formed, like the one recently discovered [20].

5 - Conclusion.

We consider two images of hypermassive objects located at the center of galaxies M87 and Milky Way, immediately identified as so-called giant black holes. Noting the identity for these two objects of the value 3 of the ratio of maximum temperature to minimum temperature, and assimilating the darkening effect of their central part, we show that these could be subcritical objects whose radius would then be $\sqrt{8/9} R_s$, such that the enormous rise in pressure towards the center would then allow it to balance the force of gravity. Anticipating the future publication of works reporting, in a bimetric model, joint fluctuations of these, modifying the apparent mass coefficient $\sqrt{\bar{g}/g}$, we evoke a possible formation scheme of such objects, resulting from the formation of a centripetal density wave, giving birth to a quasar when it reaches the center. The object Sgr A* would thus be an extinct quasar.

Références :

- [1] First M87 Event Horizon Telescope Results. I. The Shadow of the Supermassive Black Hole. K. Akiyama, A.Alberdi,W.Alef,K.Asada, R.Azulay, A.K.Backo, D.Ball,M. Balakovic, J. Barrett. Astrophysical Journal, vo. 875, n°1,2019
- [2] First Sagittarius A* Event Horizon Telescope Results. I. The Shadow of the Supermassive Black Hole in the Center of the Milky Way. K. Akiyama, A.Alberdi, W. Alef, J.C.Algaba, E. Anantua, K. Asada, R. Azulay, U. Bach, A.K.Backo. The Astrophysical Journal Letters, vol. 930, number 2. 2022. DOI 10.3847/2041-8213/ac6674
- [3] L.Medeiros,D.Psaltis,T.R.Lauer,F.Ozel : Principal-component Interferometric Modeling (PRIMO), and Algorithm for EHT Data. I. Reconstructing Images from Simulated EHT Observations. Astrophysical Journal. 943 :144 (19p), 2023, February.
- [4] K. Schwarzschild : Über das Gravitationsfeld einer Kugel Aus incompressibler Flüssigkeit nach der Einsteinschen Theorie. Sitzung der phys. Math. Klasse v.23 märz

1916. English translation, by S.Antoci. On the gravitational field of a sphere of incompressible fluid according to Einstein theory. arXiv :physics/9905030v1 [physics.hist-ph] 12 may 1999.

[5] Gravitation. C.W.Misner, K.S.Thorne, J.A.Wheeler. Pinceton University Press. 2017.

[6] Ludwig Flamm. Beiträge zur Einsteinschen Gravitationstheorie, Physikalische Zeitschrift XVII (1916) pp. 448-454.

[7] H.Weyl.Zur Gravitationstheorie. Annalen der Physik IV Fogl. 54 pp 117-145

[8] N.Kumar : On the Accelerated Expansion of the Universe. Gravitation and Cosmology. 2024-Springer Link. Vol. 30 pages 85-88. April 2024.

[9] C.Deffayet, G.Dvali, G. Gabadadze : Accelerated Universe from gravity leaking to extra dimension. Phys. Rev. D 65, 044023 (2002).

[10] L.Boyle, K. Finn, N.Turok : CPT-symmetric universe. Phys.Rev.Lett. 121, 251301 (2018)

[11] L.Boyle, K. Finn, N.Turok :The Big Bang, and beutrino daek matter. Annals of Physics. 438, 168767 (2022)

[12] S.J.Robles, Pirez : Time-reversal symmetry in cosmology and creation of a universe-antiuniverse pair.Universe 2019 (5), 150.

[13] S.J.Robles, Pirez : Quantum creation of a universe-antiuniverse pair. arXiv : 2002.09863

[14] J.P.Petit, G.D'Agostini : Negative Mass hypothesis in cosmology and the nature of dark energy. Astrophysics And Space Sccience,, A **29**, 145-182 (2014)

[15] J.P.PETIT, Twin Universe Cosmology, Astrophys. and Sp. Science, **226**, 273-307, 1995

[16] G. DAGostini and J.P.Petit : Constraints on Janus Cosmological model from recent observations of supernovae type Ia, Astrophysics and Space Science, (2018),

[17] J.P.Petit , H.Zejli : Janus Cosmological Model mathematically and Physically Consistent. Cnrs scientific data base. Hal-04583560v1halDOI 10.5281/zenodo.112377996

[18] J.M.Souriau : Structure des systèmes dynamiques. Dunod Ed. France, 1970 and Structure of Dynamical Systems. Boston, Birkhäuser Ed. 1997

[19] A.Escriva, C. Germani, R.K.Seth Universal Threshold for Primordial.Phys. Rev. D 101, 044022 13 February 2020

[20]A.M.Lopez, T.G.Clowes, G.M.Willinger. A Big Ring in the Sky. arXiv :2402.07591, 12 Feb. 2024